DOI: 10.31276/VJSTE.64(1).53-62

A review on injectable hydrogels from xanthan gum for biomedical applications

Thai Phuong Thao Nguyen[1, 2], Phuong Hien Le[1, 2], Thi-Hiep Nguyen[1, 2*]

[1]*School of Biomedical Engineering, International University*
[2]*Vietnam National University, Ho Chi Minh city*

Received 8 February 2022; accepted 11 March 2022

Abstract:

Xanthan gum (XG) is recognised as one of the most popular natural polymers extensively used today due to its biodegradable and biocompatible properties, and, therefore, XG can be used to produce hydrogels with other polymers to expand its uses. However, at present, there has not been much research on preparing injectable hydrogels from XG. Moreover, up to now, there are only a limited number of review articles related to this topic. This review will provide a well-organised and somewhat extensive presentation of previous studies that have been executed on injectable hydrogels from XG. Also, applications have been using XG to fabricate injectable hydrogels such as cartilage tissue engineering, bone tissue engineering, delivery system, and bioink will be reviewed.

Keywords: **biomedical application, injectable hydrogel, xanthan gum.**

Classification number: **3.6**

Introduction

Biomaterials cover a wide spectrum of materials from metallic orthopaedic implants to polymeric constructs-all of which are used to replace, restore, or regenerate missing tissue structure and/or function. Polymeric hydrogels, traditionally understood as three-dimensional (3D), are water-swollen polymer networks generated via physical or chemical crosslinking is an ever-increasing class of biomaterials. They have been extensively explored for countless biomedical applications due to advantages such as oxygen and nutrient permeability, biocompatibility, physical characteristics like those of the native ECM, and adjustable physical and mechanical characteristics [1].

Nevertheless, the use of pre-formed hydrogels at a desired spot in the body necessitates an intrusive surgical process that can bring discomfort and pain, heavy bleeding, infection, nerve damage, as well as a prolonged recovery time of the patient. As a result, their clinical utility is restricted. Hence, to overcome these drawbacks of pre-formed hydrogels, recent hydrogel research has focused on injectable hydrogels defined as hydrogels undergoing the transition from sol to gel under environmental conditions at the injection site. Injectable hydrogels not only possess the benefits of traditional hydrogels, but they also have superior properties such as the ability to be injected into target sites with little invasiveness and the capability of filling oddly shaped defect sites. As a result, they have emerged as a potential and effective material system for a variety of biomedical applications including the delivery systems for therapeutic agents delivery like cells, drugs, and bioactive molecules to cure infectious and inflammatory diseases as well as cancers, and even the repair and restoration of tissues like muscle, bone, skin, and cartilage [2].

Natural and synthetic polymers are commonly used to fabricate hydrogels. Recently, there has been an upsurge of demand for cheaper biodegradable and biocompatible non-toxic products with natural polymers taking precedence over synthetic polymers. XG is recognized as a natural polymer that is extensively used today due to excellent biodegradability and biocompatibility; therefore, XG can be used to produce hydrogels with other polymers to expand its uses [3, 4]. However, at present, there has not been much research on preparing injectable hydrogels from XG. Therefore, in this review, studies of injectable hydrogels from XG will be presented in a well-organised and extensive manner. Also, the applications of XG-based injectable hydrogels such as cartilage tissue engineering, bone tissue engineering, delivery system, and bioink will be reviewed.

Structure and properties of XG

Structure

XG is an anionic exocellular polysaccharide mainly produced from the Gram-negative bacteria *Xanthomonas campestris*. The structure of XG is primarily made up of repeating pentasaccharide units including two D-glucose units, two D-mannose units, and one D-glucuronic acid unit [5] (Fig. 1). A pendant trisaccharide side chain including a D-glucuronic acid unit between two D-mannose units is attached to the O-3 position of D-glucose units by α-1,3 linkages. The terminal β-D-mannose is linked to the O-4 position of the β-D-glucuronic acid, which is successively linked to the O-2 position of an α-D-mannose. There are groups

*Corresponding author: Email: nthiep@hcmiu.edu.vn

of acetates and pyruvates of varying amounts attached at the two D-mannose units, which depend on the bacterial strain, the conditions of fermentation, and chemical modifications [6].

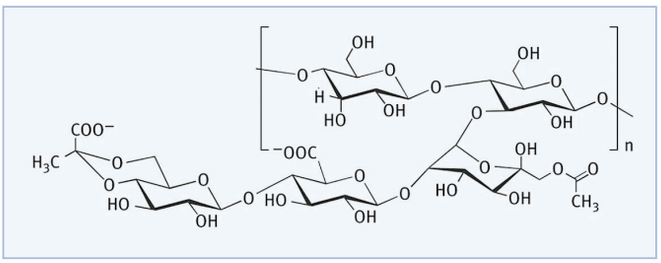

Fig. 1. Structure of XG.

XG has two molecular conformations including helical/ordered conformation and random coil/disordered conformation. Right-handed five-fold helix conformations are stabilised by non-covalent interactions between the side chains of the trisaccharide and the backbone of the chain and are destabilised by electrostatic attraction between carboxylate groups. Consequently, XG can undergo order-disorder conformation transitions (Fig. 2) if the temperature or ionic strength is changed. Random coils can be formed under high temperature or low ionic strength whereas high ionic strength or low temperature can stabilise the order conformation resulting in an extraordinarily stable XG, which commonly manifests as a dimeric or double-stranded chain. As a result of this behaviour, XG alone can form a weak gel when prepared at a concentration higher than the critical concentration of approximately 0.3% w/v [7].

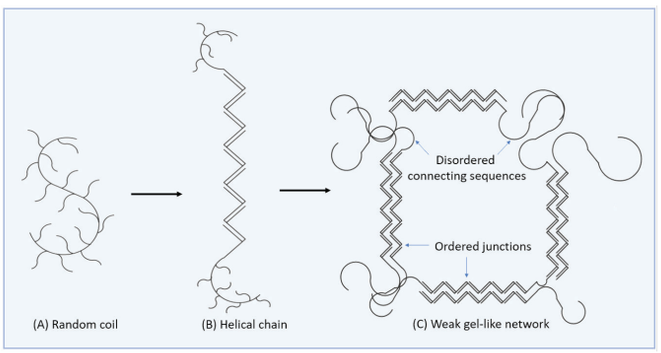

Fig. 2. (A) The disordered conformation of XG, (B) the ordered conformation of XG, and (C) the lateral association of ordered chains to form a weak gel-like network.

Properties

Viscosity and rheological properties: XG shows a high solubility in both cold and hot water, which is due to the polyelectrolyte structure of XG molecules. XG solutions are highly viscous even at low polymer concentrations, which contribute to its excellent suspension and thickening properties [8]. XG solutions exhibit the behaviour of non-Newtonian fluids and a highly pseudoplastic property of which its viscosity declines speedily as the shear rate increases. Fig. 3 presents how the XG polymer network is influenced by mechanical shear being applied and removed. When the yield stress is surpassed, XG solutions become pseudoplastic. The network then disassembles with individual polymer molecules positioning themselves in a straight line along the shear force direction. The level of the disassembly is commensurate with the shear rate. Once shear is no longer applied, the network will promptly reorganise. At adequate concentrations of XG, it looks almost gel-like at rest, yet, they can easily be pumped or mixed [9].

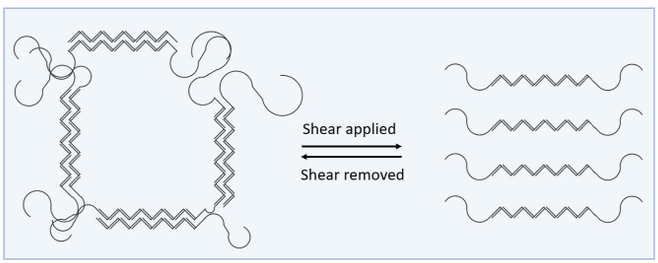

Fig. 3. Effect of shear on the polymer network of XG.

Influence of pH on the viscosity of XG: the viscosity of an XG solution is practically constant as pH changes between 1 and 13. XG is steadily deacetylated at pH>9 [10], while at pH<3 it loses the pyruvic acid acetal groups [11]. Neither deacetylation nor depyruvylation significantly affect XG solution viscosity since the rheological properties of deacetylated or depyruvylated XG are similar to those of native XG [8]. However, pH variations will affect changes in the reduced viscosity of XG solution. At pH values of 2.5 and 3.5, XG solutions exhibit straight decreasing lines of the reduced viscosity with dilution, which represents the behaviours of neutral polymers. This can be clarified based on the protonation of carboxylic groups in an acid medium, where XG chains carry no charge and are partially flexible. The carboxylic groups within a weak acid medium are incompletely protonated (pH=4) or entirely deprotonated (pH=6) [12]. At pH=5, carboxylic groups on the side chain of XG create electrostatic repulsive forces that cause the chain to enlarge and make the reduced viscosity amplify constantly alongside the dilution of the polymer. When an XG solution is at a high dilution in water, a polyelectrolyte effect can be implied from the upward curvature [13].

Effect of electrolytes on the viscosity of XG: fluid in the human body contains an enormous amount of electrolytes that are supposed to change the solvation sphere around biodegradable materials. If the environment is negatively affected by the electrolytes and becomes disadvantageous for the diffusion of water molecules into biodegradable polymers, then its properties of degradability should reflect this. The viscosity of an XG solution is mainly dependent on gum concentration. The effects of electrolytes have little impact on XG. Under 0.15% w/v gum concentration, a small amount of an added electrolyte like sodium chloride can slightly reduce the viscosity. This is because the addition of electrolyte reduces the electrostatic forces between XG molecules resulting in less availability

in the XG molecular network [14]. In other words, the helical conformation of XG seems to be stabilised by the low level of electrolyte concentration, which also downgrades the carboxylate anions' electrostatic repulsion (Fig. 4). However, the addition of electrolytes acts in the opposite manner at higher concentrations of gum. Electrolyte addition marginally increases the solution viscosity until reaching a peak at 0.02-0.07% w/v concentration of sodium chloride; however, additional salt has little or no impact on viscosity above this level, which is due to the enhanced interactions between salt molecules and XG molecules. Thus, the viscosity of an XG solution will be independent of the salt if the salt amount exceeds 0.1% w/v [15].

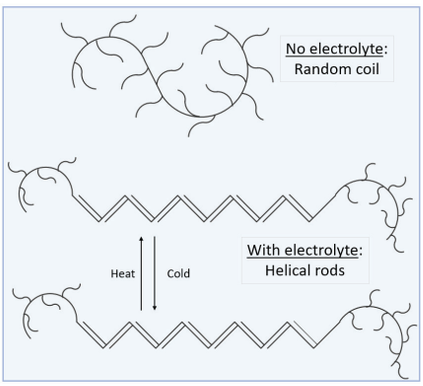

Fig. 4. Effect of electrolyte on XG molecular conformation.

Influence of temperature on the viscosity of XG: XG solutions are affected by two characteristic temperatures including the measurement temperature (T_M, the temperature when the viscosity is measured) and the dissolution temperature (T_D, the temperature when XG is dissolved). The viscosity of XG solutions decrease when T_M increases. Alternatively, there is a decrease in XG viscosity when T_D is raised up to 40°C. From T_D=40 to 60°C, XG viscosity increases with an increase in temperature. XG solutions exhibit this behaviour because the XG conformation will go through an ordered-disordered state change as T_D shifts from low to high (Fig. 2). This results in an increase in XG molecule hydrodynamic volume and, thus, gives rise to the viscosity. For T_D above 60°C, the viscosity decreases with an increase in temperature [8].

Effect of enzymes and oxidants on the stability of XG: XG cannot easily be affected by most degradation by microorganisms; however, it can somewhat be vulnerable to cellulase in the disordered conformation. On the other hand, XG can be completely biodegradable, which means it can be depolymerised by enzymes produced by certain microorganisms when certain environmental conditions are met. Additionally, like other gums, XG is susceptible to degradation by strong oxidising agents such as persulfates and peroxides [15].

Biocompatibility of XG: a well-known attribute of XG is its excellent biocompatibility, non-toxicity, and intrinsic ability as an immunological agent since XG alone does not adversely affect the viability of rabbit chondrocyte cells [16]. Moreover, in vitro and in vivo studies with the fibroblast cell line L-929 showed good biocompatibility for hydrogels prepared by a combination of XG with other polysaccharides as chitosan (CHT) [17].

Fabrication of XG-based injectable hydrogels

There have been several studies on fabricating injectable hydrogels from XG. It can be seen from those studies that there are three approaches typically applied. The first approach is to purify and use XG alone to inject directly into the injection site due to its shear-thinning properties. In addition, thanks to its large number of functional groups, XG can be combined with other polymers through the second approach - via physical crosslink, and the third approach - via chemical crosslinking to fabricate injectable hydrogels.

Purified XG for direct injection

Due to the shear-thinning property, XG alone can be directly injected through a needle to the target site of the body. For example, G. Han, et al. (2012) [18] investigated the ability of intra-articular (IA) injection of XG into rabbits' knee joint. In this case, using conventional XG types (with unguaranteed purity and unknown protein and endotoxin content) would affect the accuracy of the XG injection's evaluation. So, to accurately evaluate XG for IA injections, the test sample XG needs to have high purity, high viscosity, low protein-content, and be endotoxin free. The procedure of making purified XG is illustrated in Fig. 5. He began with XG fermented broth, brought it through a precipitation step, and then through a purification process including the combination of cake filtration, enzymatic treatment, active carbon absorption, and repeated isopropanol precipitation methods in order to obtain good quality XG. This purification process, especially the enzyme treatment, helps eliminate undissolved matter and impurities such as proteins, fats, or bacterial cell residues contained in the XG fermented broth [18].

The process of enzyme treatment is preferably at a temperature of 50 to 60°C, at a pH range from 6.5 to 7.5, for about 30 min to 2 h. In terms of productivity, a temperature below 40°C is not recommended since a resulting lowered enzymatic activity would involve more than 6 h of treatment time. Enzyme deactivity can also be triggered by high temperature, causing the treatment to become ineffectual. Acidity lower than pH 6.0 would disable alkaline protease, while pH above this range is also unwanted as it can devolve the product's physical properties. If the protease concentration is too low, a satisfactory effect would not be achieved even when the treatment time is extended. Conversely, it is not advisable for the protease concentration to exceed 500 ppm by reason of creating higher costs in production without producing any further improvements. So, the process is preferred to be conducted at relatively neutral pH and at a mild temperature such that protease will exhibit an acceptable activity level to purify the XG solution [19].

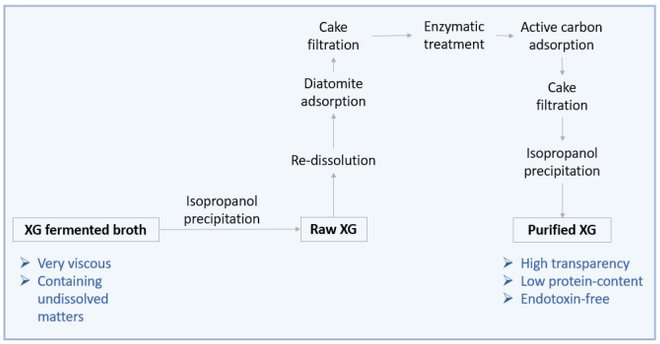

Fig. 5. Schematic procedure of making purified XG.

The final product contained 99.6% of XG, which indicated that it met the initial requirement of high purity. Moreover, the purified XG contained no proteins and no endotoxins. Finally, the acquired IA injection of XG was observed to be transparent, highly viscous (1597±32 mPas), and heat stable (could be sterilized at 121°C for 15 min) [18].

Polymers combined with XG via physical crosslinks to fabricate injectable hydrogels

Hydrogels that are physically crosslinked undergo the gel state by altering intermolecular forces like electrostatic ionic repulsion, hydrophobic interaction, hydrogen boding, or intermolecular assemblies like complementary binding, stereo-complexation, and guest-host inclusion. These changes can be caused by the internal organization of the polymers or stimulated by external stimuli such as pH, heat, or the presence of certain molecules [20]. Physical crosslinking methods are easy and safe ways to prepare injectable hydrogels since they do not require the use of potentially harmful crosslinkers or catalysts.

Having prepared injectable hydrogels based on XG and methylcellulose (MC) via thermo-induced interaction, Z. Liu, et al. (2015) [21] later described that a blended solution of the two polymers instantly retrieved its high viscosity and promptly created a hydrogel at body temperature. MC is a water-soluble cellulose derivative that can induce a sol-gel transition guided by hydrophobic interactions that depend on temperature changes. At 23°C, the XG/MC blend carries only the XG network interfered with MC molecules, which is the reason why the combination at 23°C has the behaviour of shear-thinning, but the viscosity is not as high as that of solution containing only XG. When the temperature is raised to 37°C, intermolecular hydrophobic interactions trigger the XG/MC blend solution to form gels so it possesses the double networks of XG and MC at the same time (Fig. 6). With the rat's body being analysed in terms of biocompatibility, elimination, and gelation, the proportion of hydrogel grew in the first week of post-injection because of swelling, which then slowly decreased until the 36th day after injection when it finally disappeared. The inflammatory cells in the tissues were monitored around the implanted XG/MC hydrogel and the signs of inflammation decreased as the duration of implantation increased In addition, on the 27th day after injection, inflammation of the cells practically disappeared and the histology of the tissues around the site was entirely recovered 37th days post-injection [21].

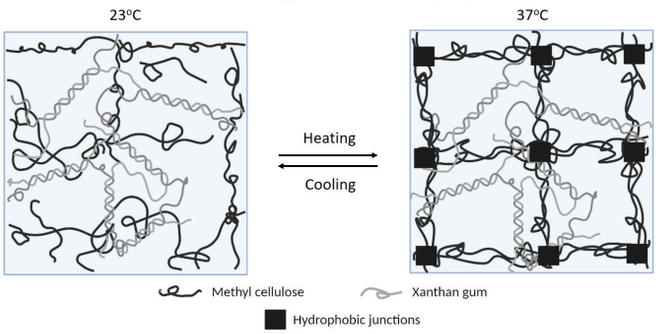

Fig. 6. Gelation mechanism of XG/MC hydrogels.

Additionally, XG can also be combined with pluronic F127 (PF127) to fabricate injectable hydrogels through hydrophobic interaction and hydrogen bonding. PF127, a triblock copolymer comprised of poly (ethylene oxide-b-propylene oxide-b-ethylene oxide or PEO-b-PPO-b-PEO), can undergo a sol-gel transition at around 20-25°C depending on the concentration of the copolymer [22]. The gelation of PF127 occurs owing to its dehydration, which forces this substance to be constructed with micelle subunits where the core of which is made up of hydrophobic PPO blocks and the shell is made up of hydrophilic PEO chains (Fig. 7A). However, the low sol-gel temperature and thermo-reversible property of PF127 make this substance inconvenient and difficult to fabricate stable hydrogels. Therefore, different PF127-based formulations combined with XG were modulated to create a stable *in-situ* gel and ensure gelation at around 37°C. In the viscosity studies, XG/PF127 *in-situ* gel revealed a rise in temperature and concentration that was dependent on viscosity. The viscosity of the *in-situ* gel rose as the micelle concentration rose because of the intermicellar distance being shortened. Furthermore, the increase of XG concentrations from 0.2 to 0.6% also made the viscosity of *in situ* gels decrease. This is a consequence of the electrostatic repulsion of the charged groups where XG chains are substantially stretched at room temperature and create helical structures through hydrogen bonding. As the temperature rises, the lengthy chains of XG form a coil-like conformation (Fig. 7B). In the situation of *in-situ* gels, the lengthy XG chains infiltrate across distinct copolymer micelles and interact with PEO corona, which ensures a higher degree of elasticity and high viscosity to the resultant gel (Fig. 7C) [23].

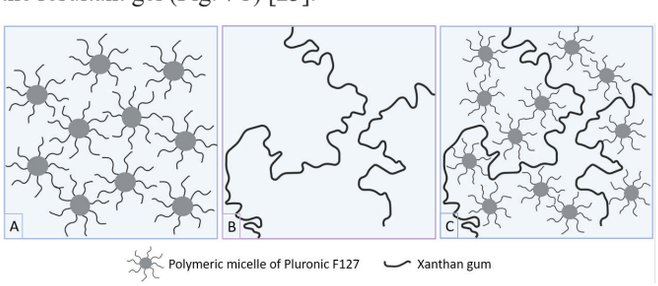

Fig. 7. (A) PF127 hydrogel, (B) XG solution, and (C) XG/PF127 hydrogel at 37°C.

In another research works, XG was combined with gellan gum (GG) to create an *in situ* gelling system via temperature and ionic gelation mechanism with Ca^{2+} ions or DMEM supplemented as the supply of cations for gelation [24, 25]. GG, an anionic extracellular polysaccharide, appears in a random coil shape when dissolved in water at temperatures over 80°C, which transforms to a double-helix structure when cooled, followed by self-assembling and the production of oriented bundles [26]. Cations aid in the creation of a stable gel by assisting in the linking of the bundles. The creation of double helical junction zones and the later aggregation of the double-helical segments lead to a 3D network via cation complexation and hydrogen bonding with water [27] (Fig. 8). The combination of XG and GG demonstrated a shear-thinning effect at various shear stresses for all of the tested concentrations, indicating that the hydrogel was easy to inject. This was due to the shear force at the interface of the needle and tissue, which allows the gels to shear-thin and then flow into the defect site. The polymer solution returns to its gel state after the shear stress is removed, suggesting that the hydrogel could be provided through injection. Measurements of viscosity versus temperature validated the gelation temperature being between 37 and 40°C for all tested concentrations, with the onset of gelation at roughly 42°C.

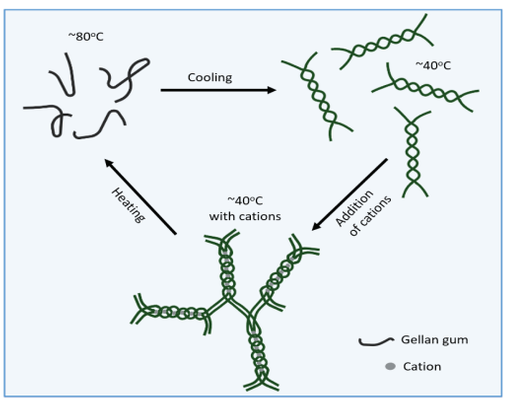

Fig. 8. Gelation mechanism of GG.

Another polymeric combination belongs to XG and konjac gum (KG), which was investigated to study its printing properties [28]. In XG/KG hydrogels, A. Abbaszadeh, et al. (2016) [29] hypothesised two forms of interaction (type A and type B) (Fig. 9). As for type A, XG maintains helical conformations and the produced hydrogel melts at a lower temperature range (from 30 to 45°C). In a type B interaction, the 2-fold structure of disordered XG is accountable for the synergistic binding with KG. Backbone-to-backbone development of junction zones causes the contact and the resulting gel melts at a higher temperature of around 60°C. Changes in ambient parameters such as functional group content, pH, and ionic concentration can affect the XG transition temperature, which is a critical parameter in defining the type of contact [29]. The XG/KG mixture with the addition of syrup investigated in work of [28] had an interaction type A with a melting temperature of around 45°C. The printing temperatures investigated had a significant impact on the rheological features of the hydrogels, which imply a distinct type of interaction. In terms of temperature, changes in elastic modulus (G′) were more connected than those of viscous modulus (G″). Printed samples at 50°C had lower G' values than those at 25°C, which indicates less elasticity at 50°C. In terms of the effect of composition on rheological characteristics, mixtures with lower syrup concentrations but higher XG and KG values had higher G′, G″, and η* values [28].

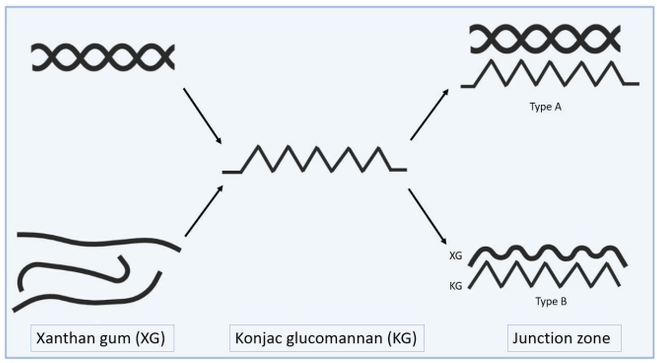

Fig. 9. Mechanisms for the interaction between XG and KG.

CHT, a linear cationic polysaccharide, can be combined with XG to generate injectable hydrogels via electrostatic attraction or ionic interaction between the amino groups of CHT and carboxyl groups of XG [30] (Fig. 10). CHT molecules contain positive charges at low pH, which combine with negatively charged polyions of XG to create polyelectrolyte complexes [31]. J. Kim, et al. (2017) [32] prepared XG/CHT-based polyelectrolyte hydrogels having a viscoplastic behaviour that satisfies all the rheological models like the Bingham, Herschel-Bulkley, Power law, modified-Bingham, and modified Herschel-Bulkley, as well as Casson models as a non-Newtonian material.

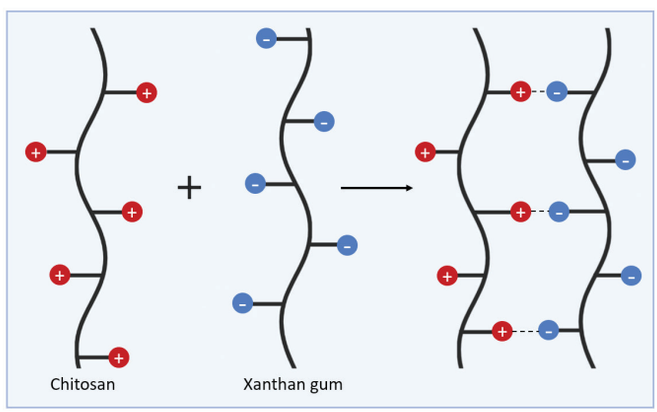

Fig. 10. Illustration of ionic interaction of CHT and XG.

Polymers combined with XG via chemical crosslinks to fabricate injectable hydrogels

Chemically crosslinked hydrogels are a type of hydrogel that can transition from liquid to gel state by chemically creating new covalent bonds in the polymer network. Reactions can

be triggered by a variety of processes such as click chemistry, Schiff base reactions, Michael reactions, enzymatic reactions, photo-polymerization, disulphide-forming reactions, or redox reactions. From these reactions, newly created covalent bonds build a polymeric 3D network structure that can trap water and encapsulate living cells or therapeutic agents.

In the preparation of an injectable hydrogel combining CHT and oxidized XG (OXG) via Schiff base reaction between free amine groups on CHT and aldehyde groups on OXG (Fig. 11), the observed swelling capacity was not much different among the three ratios used in the preparation of CHT/OXG hydrogels (CHT/OXG=80/20; 70/30; 75/25). This was believed to be due to the small crosslinks of the structure and tighter intramolecularly, and thus lower swelling ratios [33]. Critical strain for 80/20 and 75/25 CHT/OXG hydrogels was around 10%. However, when the OXG concentration was increased in the 70/30 CHT/OXG hydrogel, the critical strain was found to be roughly 2.52%, indicating that the linear viscoelastic zone was at a lower strain at this ratio. In the tests of gelling time and gel fraction, it was proved that when the volume ratio of OXG was raised, the gelling time lowered, and the gel formed was comparatively more stable. The 70/30 ratio hydrogel had the fastest gelation time of about 18 s suggesting that the crosslinking was higher and the gels were becoming stronger and more stable over time. In another study about the preparation of an injectable hydrogel from OXG and carboxymethyl chitosan (NOCC) via Schiff base reaction, the hydrogel with a mass ratio of 1/0.33 (OXG/NOCC) had the fastest gelation time of 10±5 s. Moreover, the 1/0.33 ratio hydrogel also had the highest swelling ratio compared to all the samples, was stable, and had a viscoelastic solid-like behaviour [34].

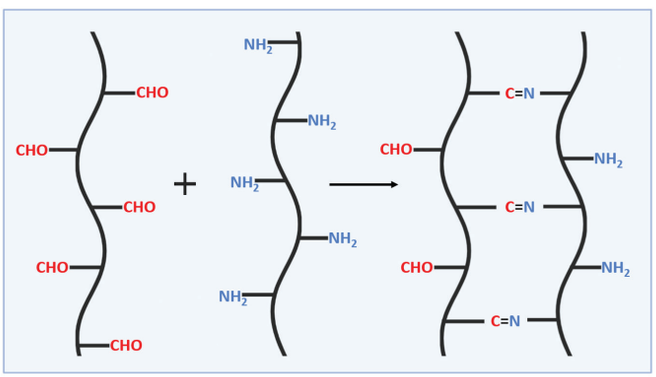

Fig. 11. Schiff base reaction between aldehyde groups and amine groups [35].

An injectable hydrogel from XG, silk fibroin (SF), and sodium trimetaphosphate (STMP) with ion conductivity was prepared in previous research [36]. SF, a high molecular weight disulphide-linked block copolymer, has been used to create hydrogels with great mechanical strength and biocompatibility [37]. STMP, a water-soluble and non-toxic crosslinker, is used in food and medicine, for example, as a chemical crosslinking agent to make polysaccharide hydrogels or to induce phosphorylation, which improve the functional characteristics of proteins and sugars. The blending of XG, SF, and STMP produces hydrogels with the characteristics of swelling but water insoluble. The viscosity of a XG/SF/STMP hydrogel is mostly determined by XG since XG/STMP and XG/SF/STMP gels both contain 3 wt% XG and had very identical viscosity-shear rate curves. All XG/SF/STMP hydrogels have a viscosity that decreases significantly with the rise of shear rate, which indicates a shear-thinning property. Additionally, with 3 wt% XG, the addition of SF particles to withstand deformation against compressive stress improved the stiffness of XG/SF/STMP hydrogels compared to XG/STMP hydrogels. Moreover, the hydrogels regained their initial values of storage moduli after being relieved of excessive strain in rheological investigations, which suggests a self-healing property in the XG/SF/STMP hydrogels. The XG/STMP and XG/SF/STMP hydrogels' ionic conductivity was equal to that of PBS [36]. In another study, R. Zhang, et al. (2018) [38] created novel injectable hydrogels with self-healing properties from XG, TM3a, and STMP. TM3a, a coded hyperbranched polysaccharide, was chemically crosslinked with XG using STMP as crosslinkers via an esterification reaction between the -OH groups of XG, TM3a, and STMP (Fig. 12). According to oscillatory rheological tests, chemical crosslinking occurred quickly after mixing STMP solutions into XG-TM3a solutions, and the crosslinked network developed gradually over time. From the beginning of the rheological tests, the storage modulus was far ahead of the loss modulus, and these moduli increased slowly during the experimental period. Moreover, XG/TM3a/STMP hydrogels shown a self-healing property when a large and small amplitude oscillation was applied one at a time. Furthermore, XG/TM3a/STMP hydrogels also show a shear-thinning behaviour, which make XG/TM3a/STMP hydrogels an ideal candidate for forming injectable hydrogels or for 3D printing.

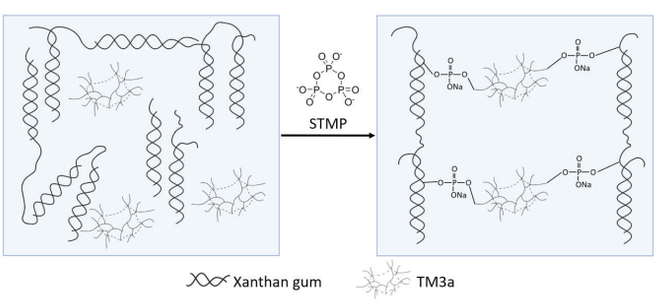

Fig. 12. Illustration of XG/TM3a/STMP hydrogels' synthesis.

Another study used intermolecular crosslinking between OXG and 8-arm poly (ethylene glycol) (PEG) hydrazine via hydrazone links to create an injectable hydrogel with self-healing property (Fig. 13). According to recorded data, a greater PEG hydrazine concentration prompted greater elasticity, which means these hydrogels were more likely to endure the formulation and delivery strains as an injectable formulation. The findings from the thixotropic test revealed that even though hydrogels developed quickly, they were effortlessly extrudable

when passing through the needle and instantly regained their viscoelastic gel properties. To comprehend the self-healing properties of hydrogels, their tendencies to seamlessly heal themselves into union when violently cut into two separate pieces were explored via rheological studies and a visual method. It was found that hydrogels recovered instantly after being relieved of excessive strain in rheological investigations. This is due to the use of dynamic hydrazone linkages to generate hydrogels. In the visual method, there were no obvious seams observed indicating that the two pieces had healed properly. Research on self-healing ability were also performed on hydrogels fabricated at different pH values. The results showed that gels fabricated at a mildly acidic pH had more efficient drug/dye distributions than gels tested at neutral pH [39].

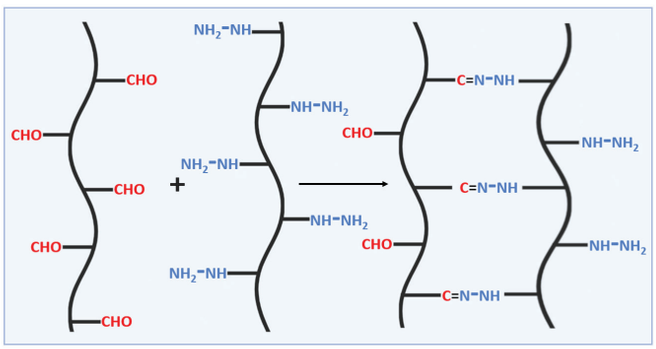

Fig. 13. Hydrazone linkage between aldehyde groups and hydrazide groups [35].

Applications of XG-based injectable hydrogels

Cartilage tissue engineering

OA occurs because of chondrocyte apoptosis. The excessive expression of mediators causing inflammation like nitric oxide (NO), tumour necrosis factor-α (TNF-α), interleukin-1 (IL-1), and prostaglandin E2 (PGE2) in serum or in synovial fluid causes chondrocyte apoptosis. The poor proliferative potential of chondrocytes after injury or during the healing process complicates cartilage regeneration. In cases of osteoarthritis, cartilage tissue engineering plays the most important role in overcoming these obstacles [40].

IA injection of XG is proven to treat OA better than hyaluronic acid (HA) since no statistically significant differences on OA were observed for the effects of chondro-protection by IA injection of XG and HA [18]. Also, the preliminary cytotoxicity effects of XG on rabbit chondrocytes regarding proliferation and protein expression of matrix metalloproteinases (MMPs) and tissue inhibitors of metalloproteinase-1 (TIMP-1) in chondrocytes induced by IL-1β were assessed. Down-regulating MMPs and up-regulating of TIMPs (or MMPs inhibitors) are rational targets for treating OA since the imbalance between MMPs and TIMPs play an important role in the development of OA. In experiments using various doses of XG with and without IL-1β, the results showed that XG alone did not cause adverse effects on the viability of chondrocyte cells, and also significantly reversed the IL-1β-induced reduction of the proliferation of chondrocyte cells. Additionally, XG increased TIMP-1 expression in a dose-dependent manner while inhibiting MMP release produced by IL-1β [16] (Fig. 14). XG does not exhibit any cytotoxicity on the chondrocyte cells of rats and has effects on the ATDC5 cells' Wnt3a/β-catenin signalling [41]. In addition, an injection of low molecular weight XG (from 1×10^6 to 1.5×10^6 Da) could protect cartilage tissue from damage, reduce the concentration of NO in the synovial fluid, and was able to reverse the amplification of knee joint width similar to high molecular weight (HMXG) [42]. LWXG promotes chondrocyte proliferation while decreasing apoptosis at the cellular level. These effects are evoked via down-regulation of the protein levels of caspases-3 and bax (an apoptosis inducer) and via up-regulation of protein levels of bcl-2 (apoptosis inhibitor) in cartilage both *in vitro* and *in vivo* [43]. Furthermore, the combination of XG with CHT to form an injectable hydrogel is an excellent scaffold for cartilage regeneration. The hydrogel has been proven to provide a static environment that enables cells to maintain their chondrogenic phenotype while allowing unimpeded diffusion of nutrients and waste materials for every cell during the culture periods [33].

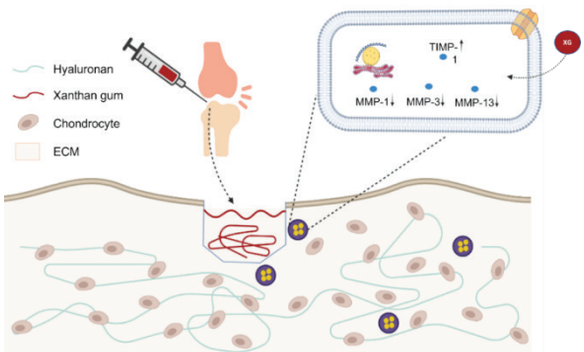

Fig. 14. IA injection of XG could increase the expression of TIMP-1 and down-regulate the expression of MMP-1, MMP-3, and MMP-13.

Bone tissue engineering

Bone defects have risen to the top of the list of causes of illness and disability among the elderly around the world. Even when autografting is seen as the benchmark repair method of bone defects, it is constrained by donor-site illness and unknown side effects. As a result, bone tissue engineering has piqued researchers' interest as a viable technique for fixing bone defects without the drawbacks and restrictions of bone allografts, xenografts, or autografts [44]. Injectable hydrogels are at an advantage over other materials since they can adjust to the defect's edges and can be inserted into deep defect sites with little invasiveness. As a result, injectable hydrogels can significantly minimize surgery duration, scar creation, post-operative discomfort (due to the fact that fewer muscles are affected during surgery), and recovery time [45]. Additionally, most hydrogels can imitate the native ECM, which allow cells to multiply and develop in a favourable

environment [46]. By incorporating growth factors, along with different osteoinductive components, can further help to improve the treatment's outcome [47].

D. Dyondi, et al. (2013) [25] used a dual growth-factor system to enhance the development of foetal osteoblast cells in the human body using injectable XG/GG hydrogels with CHT nanoparticles, basic fibroblast growth factor (bFGF), and bone morphogenetic protein 7 (BMP7). Due to the prolonged release of growth factors, XG/GG hydrogels combined with nanoparticles demonstrated a considerable improvement in cell proliferation and differentiation. When compared to hydrogels consisting of a single growth factor, dual growth factor hydrogels had more calcium deposition and alkaline phosphatase. In this experiment, the viability of L929 mouse fibroblast cells was higher than 95%, while the viability of human foetal osteoblast cells was reported to be 80% with XG/GG hydrogels as measured by the MTT assay for 48 h. Furthermore, in implant failure, XG/GG hydrogels shows antibacterial activity against common infections such as Pseudomonas aeruginosa, Staphylococcus epidermidis, and Staphylococcus aureus. In addition, D. Dyondi, et al. (2011) [24] had previously investigated the synergistic effect of platelet-derived growth factor BB (PDGF-BB) and basic fibroblast growth factor (bFGF) encapsulated inside an injectable porous hydrogel derived from XG and GG. The results show that there was an increase in the amount of total protein synthesis from osteoblasts and the amount of collagen in hydrogels that contained bFGF and PDGF by the 21st day.

Delivery system

The use of injectable hydrogels as a system or a carrier in the process of delivering cells, bioactive molecules, drugs, and other therapeutic agents is another common application. In addition to possessing properties that make hydrogels widely used for the delivery purposes (such as possessing a water-swollen porous structure that offers a suitable environment for cells, bioactive molecules, and also permitting for their controlled release), injectable hydrogels have several other benefits within the range of this application such as minimal invasive administration and better homogeneous encapsulation [35].

A previous study demonstrated that an injectable hydrogel containing an XG/MC combination could be a suitable long-term medication delivery strategy since it showed sustained release behaviour when loading with an anthracycline anticancer drug named doxorubicin (DOX). Longer release occurs with higher DOX concentration. Moreover, the loaded DOX would be released faster *in vivo* via hydrogel degradation [21]. Additionally, J. Huang, et al. (2018) [34] created an *in situ*-forming hydrogel for local drug delivery based on OXG and NOCC. According to the releasing assay of bovine serum albumin-fluorescein isothiocyanate (BSA-FITC, a model drug), the OXG/NOCC hydrogel could provide a stable and uninterrupted drug release for 10 h. After 20 h, the BSA-FITC releasing ratio was over 80%. Moreover, in comparison to conventional injectable fibrin gel, the OXG/NOCC hydrogel had the advantage of avoiding drug eruption in liquids, which was beneficial for wet wounds. Besides, the controlled release properties of hydrogels derived from XG, TM3a, and STMP were also investigated. The diffusion kinetic profiles of BSA and 5-Fu (model drugs) from the hydrogels revealed that the BSA-loaded and 5-Fu-loaded XG/TM3a/STMP hydrogels displayed a controlled release behaviour at a slower rate and reaching a maximum after being placed on a platform, which indicated that the BSA and 5-Fu diffused moderately and in a prolonged manner into the PBS medium [38]. Furthermore, several other XG-based injectable hydrogels have also been evaluated for delivery applications. The XG/CHT-based polyelectrolyte hydrogels for the delivery of Chlorhexidine (CHX), an antiseptic agent that has been used in dental therapies for gingival inflammation and plaque control, may be useful for acute or chronic periodontitis [32]. The XG/SF/STMP hydrogels containing BSA as a drug model could be used as drug carriers with the property of controlled release while having 59.1% of BSA cumulative release ratios into PBS medium [36]. A prepared XG/PF127 *in situ* gels containing methotrexate (MTX), the most used disease-modifying anti-rheumatic drug, shows to be a promising drug delivery system that could minimise the dose and dosing frequency, and was also predicted to be an effective IA drug delivery that could treat rheumatoid arthritis [48].

Bioink

Bioink, or 3D printing, enables the production of personalised tissue-engineered products with high tunability and complexity. Printable and biocompatible hydrogels are attractive materials for 3D printing applications because they offer favourable biomimetic environments for live cells such as high water content, porous structure, bioactive molecule incorporation, and tuneable mechanical properties and degradation rates. An ideal 3D printing gel would have a well-defined network, sufficient gel strength, appropriate viscosity, ability to fuse with previously printed layers, and ability to maintain its print shape [49].

In the work of synthesising 3D printing hydrogels based on XG and KG, the printing quality of 3D structures has shown to be significantly affected by the printing temperature. For the printing of a five-point star, models printed at 50^{o}C were more delicate yet well-defined than models printed at 25^{o}C. In this research, P.G. Segovia, et al. (2020) [28] did the optimisation with the goal of increasing the figure's height after 5 min and 1 h while keeping the figure's area approximately 12.3 cm^2. The optimal composition obtained from the process variables for the printing of a five-points star at a printing temperature of 50^{o}C was 0.9773/0.0062/0.016 (syrup/XG/KGM). In another study, R.

Zhao, et al. (2020) [36] fabricated a printable and self-healing hydrogel ink based on SF and XG chemically crosslinked with STMP. Rheological data demonstrated that incorporation of the SF microparticles into the STMP-crosslinked XG hydrogel could be attributed to the improvement of storage modulus and viscosity. With the same concentration of XG and STMP, the hydrogel containing SF in the composition had its 3D print possess a smaller width value than the one only containing XG and STMP. This indicates that the XG/SF/STMP hydrogels were more suitable to apply as an injectable material for fibre forming or 3D bioprinting with better shape fidelity of the printed structures than the XG/STMP hydrogel.

Conclusions

To sum up, XG is an outstanding natural polymer in terms of good water solubility, excellent biodegradability, and biocompatibility that can be applied for injection purposes following purification due to shear-thinning properties. Additionally, XG has been shown to be able to crosslink with other polymers by physical or chemical crosslinking mechanisms. The physical crosslinking mechanism allows XG to combine with other polymers via ionic interactions, hydrophobic interactions, hydrogen bonding, or heat-induced effects. Chemical crosslinking allows XG to bind to polymers through covalent bonds created by the Schiff base reaction, esterification reaction, and via hydrazone linkages. As described in this review, XG-based injectable hydrogels have been successfully applied in areas such as bone and cartilage tissue engineering, delivery systems for biomolecules, and bioink; however, the amount of research on these applications or other areas of biomedicine is still limited. As a result, current trends in the usage of XG-based injectable hydrogels in several biomedical applications are thoroughly examined in order to gain a better knowledge of this polymer in this field. From this review, it proves to have a promising future with the role of a biopolymer in accentuating the excellent features of tissue engineering products. Furthermore, the properties of gelling and shear-thinning possessed by XG may be more advantageous in 3D bioprinting of tissue scaffolds, and this shall set a firm ground for practical uses of tissue engineering in the future.

ACKNOWLEDGEMENTS

The authors would like to thank the authors whose works have been cited in this article. This work was funded by Ministry of Science and Technology of Vietnam under grant number: DTDL.CN-54/21.

COMPETING INTERESTS

The authors declare that there is no conflict of interest regarding the publication of this article.

REFERENCES

[1] J.H. Lee (2018), "Injectable hydrogels delivering therapeutic agents for disease treatment and tissue engineering", *Biomaterials Research*, **22(1)**, pp.1-14.

[2] M.D. Baumann, et al. (2009), "An injectable drug delivery platform for sustained combination therapy", *Journal of Controlled Release*, **138(3)**, pp.205-213.

[3] N. Kayra, A.O. Aytekin (2009), "Synthesis of cellulose-based hydrogels: Preparation, formation, mixture, and modification", *Cellulose-Based Superabsorbent Hydrogels*, DOI: 10.1007/978-3-319-76573-0_16-1.

[4] F. Ullah, et al. (2015), "Classification, processing and application of hydrogels: a review", *Materials Science and Engineering: C*, **57**, pp.414-433.

[5] P.E. Jansson, et al. (1975), "Structure of the extracellular polysaccharide from Xanthomonas campestris", *Carbohydrate Research*, **45(1)**, pp.275-282.

[6] A. Abbaszadeh, et al. (2015), "A novel approach to the determination of the pyruvate and acetate distribution in xanthan", *Food Hydrocolloids*, **44**, pp.162-171.

[7] H. Acar, et al. (2020), "Purified salep glucomannan synergistically interacted with xanthan gum: rheological and textural studies on a novel pH-/thermo-sensitive hydrogel", *Food Hydrocolloids*, **101**, DOI: 10.1016/j.foodhyd.2019.105463.

[8] F.G. Ochoa, et al. (2000), "Xanthan gum: production, recovery, and properties. Biotechnology advances", *Biotechnology Advances*, **18(7)**, pp.549-579.

[9] A. Kumar, et al. (2018), "Application of xanthan gum as polysaccharide in tissue engineering: a review", *Carbohydrate Polymers*, **180**, pp.128-144.

[10] M. Tako, et al. (1984), "Rheological properties of deacetylated xanthan in aqueous media", *Agricultural and Biological Chemistry*, **48(12)**, pp.2987-2993.

[11] I. Bradshaw, et al. (1983), "Modified xanthan - its preparation and viscosity", *Carbohydrate Polymers*, **3(1)**, pp.23-38.

[12] V.B. Bueno, et al. (2013), "Synthesis and swelling behaviour of xanthan-based hydrogels", *Carbohydrate Polymers*, **92(2)**, pp.1091-1099.

[13] C.E. Brunchi, et al. (2016), "Some properties of xanthan gum in aqueous solutions: effect of temperature and pH", *Journal of Polymer Research*, **23(7)**, pp.1-8.

[14] R. Lochhead (2017), "The use of polymers in cosmetic products", *Cosmetic Science and Technology*, **13**, pp.171-221.

[15] K. Kang, D. Pettitt (1993), "Xanthan, gellan, welan, and rhamsan", *Industrial Gums*, **13**, pp.341-397.

[16] G. Han, et al. (2012a), "The protective effect of xanthan gum on interleukin-1beta induced rabbit chondrocytes", *Carbohydrate Polymers*, **89(3)**, pp.870-875.

[17] F. Chellat, et al. (2000), "*In vitro* and *in vivo* biocompatibility of chitosan-xanthan polyionic complex", *Journal of Biomedical Materials Research*, **51(1)**, pp.107-116.

[18] G. Han, et al. (2012b), "Preparation of xanthan gum injection and its protective effect on articular cartilage in the development of osteoarthritis", *Carbohydrate Polymers*, **87(2)**, pp.1837-1842.

[19] J.M. Kobzeff, et al. (2003b), *Process for Clarification of Xanthan Solutions and Xanthan Gum Produced Thereby*, Official Gazette of the United States Patent and Trademark Office Patents 1272(1).

[20] Y. Qiu, K. Park (2001), "Environment-sensitive hydrogels for drug delivery", *Advanced Drug Delivery Reviews*, **53(3)**, pp.321-339.

[21] Z. Liu, P. Yao (2015), "Injectable thermo-responsive hydrogel composed of xanthan gum and methylcellulose double networks with shear-thinning property", *Carbohydrate Polymers*, **132**, pp.490-498.

[22] M. Bercea, et al. (2011), "Temperature responsive gels based on Pluronic F127 and poly (vinyl alcohol)", *Ind. Eng. Chem. Res.*, **50(7)**, pp.4199-4206.

[23] M. Bercea, et al. (2013), "Rheological investigation of xanthan/Pluronic F127 hydrogels", *Rev. Roum. Chim.*, **58(2-3)**, pp.189-196.

[24] D. Dyondi, et al. (2011), "Development of a dual growth factor loaded biodegradable hydrogel and its evaluation on osteoblast differentiation *in vitro*", *MRS Proceedings*, **1312**, DOI: 10.1557/opl.2011.916.

[25] D. Dyondi, et al. (2013), "A nanoparticulate injectable hydrogel as a tissue engineering scaffold for multiple growth factor delivery for bone regeneration", *International Journal of Nanomedicine*, **8**, pp.47-59.

[26] R. Chandrasekaran, et al. (1988), "The crystal structure of gellan", *Carbohydrate Research*, **175(1)**, pp.1-15.

[27] S. Matsukawa, et al. (1999), "Hydrogen-bonding behaviour of gellan in solution during structural change observed by ^{1}H NMR and circular dichroism methods", *Physical Chemistry and Industrial Application of Gellan Gum*, **114**, pp.15-24.

[28] P.G. Segovia, et al. (2020), "3D printing of gels based on xanthan/konjac gums", *Innovative Food Science & Emerging Technologies*, **64**, DOI: 10.1016/j.ifset.2020.102343.

[29] A. Abbaszadeh, et al. (2016), "New insights into xanthan synergistic interactions with konjac glucomannan: a novel interaction mechanism proposal", *Carbohydrate Polymers*, **144**, pp.168-177.

[30] F. Chellat, et al. (2000), "Study of biodegradation behaviour of chitosan-xanthan microspheres in simulated physiological media", *J. Biomed. Mater. Res.*, **53(5)**, pp.592-599.

[31] J.H. Hamman (2010), "Chitosan based polyelectrolyte complexes as potential carrier materials in drug delivery systems", *Mar. Drugs*, **8(4)**, pp.1305-1322.

[32] J. Kim, et al. (2017), "Engineered chitosan-xanthan gum biopolymers effectively adhere to cells and readily release incorporated antiseptic molecules in a sustained manner", *Journal of Industrial and Engineering Chemistry*, **46**, pp.68-79.

[33] K. Chinchu (2019), *A Novel Chitosan Based Injectable Hydrogel for Cartilage Tissue Engineering*, Master of Philosophy Thesis, 68pp.

[34] J. Huang, et al. (2018), "Novel in situ forming hydrogel based on xanthan and chitosan re-gelifying in liquids for local drug delivery", *Carbohydrate Polymers*, **186**, pp.54-63.

[35] Q.V. Nguyen, et al. (2015), "Injectable polymeric hydrogels for the delivery of therapeutic agents: a review", *European Polymer Journal*, **72**, pp.602-619.

[36] L. Zhao, et al. (2020), "Protective effect and mechanism of action of xanthan gum on the color stability of black rice anthocyanins in model beverage systems", *Int. J. Biol. Macromol.*, **164**, pp.3800-3807.

[37] N.R. Raia, et al. (2017), "Enzymatically crosslinked silk-hyaluronic acid hydrogels", *Biomaterials*, **131**, pp.58-67.

[38] R. Zhang, et al. (2018), "Rheological and controlled release properties of hydrogels based on mushroom hyperbranched polysaccharide and xanthan gum", *Int. J. Biol. Macromol.*, **120(Part B)**, pp.2399-2409.

[39] P.K. Sharma, et al. (2018), "Hydrazone-linkage-based self-healing and injectable xanthan-poly(ethylene glycol) hydrogels for controlled drug release and 3D cell culture", *ACS Appl. Mater. Interfaces*, **10(37)**, pp.30936-30945.

[40] M. Kapoor, et al. (2011), "Role of proinflammatory cytokines in the pathophysiology of osteoarthritis", *Nat. Rev. Rheumatol.*, **7(1)**, pp.33-42.

[41] J. Li, et al. (2019), "Xanthan gum Ameliorates Osteoarthritis and Mitigates Cartilage degradation via regulation of the Wnt3a/β-Catenin signaling pathway", *Med. Sci. Monit.*, **25**, pp.7488-7498.

[42] G.-Y. Han, et al. (2014), "Xanthan gum inhibits cartilage degradation by down-regulating matrix metalloproteinase-1 and -3 expressions in experimental osteoarthritis", *Journal of Bioactive and Compatible Polymers*, **29(2)**, pp.180-189.

[43] G. Han, et al. (2017), "Low molecular weight xanthan gum for treating osteoarthritis", *Carbohydrate Polymers*, **164**, pp.386-395.

[44] A. Khojasteh, et al. (2016), "Development of PLGA-coated β-TCP scaffolds containing VEGF for bone tissue engineering", *Mater. Sci. Eng. C. Mater. Biol. Appl.*, **69**, pp.780-788.

[45] L. Zhao, et al. (2010), "An injectable calcium phosphate-alginate hydrogel-umbilical cord mesenchymal stem cell paste for bone tissue engineering", *Biomaterials*, **31(25)**, pp.6502-6510.

[46] M.W. Tibbitt, K.S. Anseth (2009), "Hydrogels as extracellular matrix mimics for 3D cell culture", *Biotechnology and Bioengineering*, **103(4)**, pp.655-663.

[47] Y. Tabata, et al. (1998), "Bone regeneration by basic fibroblast growth factor complexed with biodegradable hydrogels", *Biomaterials*, **19(7-9)**, pp.807-815.

[48] T. Das, et al. (2019), "Injectable in situ gel of methotrexate for rheumatoid arthritis: development, *in vitro* and *in vivo* evaluation", *J. App. Pharm. Sci.*, **9(5)**, pp.40-48.

[49] F.C. Godoi, et al. (2016), "3d printing technologies applied for food design: status and prospects", *Journal of Food Engineering*, **179**, pp.44-54.